Spectral properties of distance matrices

E Bogomolny, O Bohigas and C Schmit

Laboratoire de Physique Théorique et Modèles Statistiques, Université de Paris XI,
Bât. 100, 91405 Orsay Cedex, France

Abstract
Distance matrices are matrices whose elements are the relative distances
between points located on a certain manifold. In all cases considered here all
their eigenvalues except one are non-positive. When the points are uncorrelated
and randomly distributed we investigate the average density of their eigenvalues
and the structure of their eigenfunctions. The spectrum exhibits delocalized and
strongly localized states that possess different power-law average behaviour.
The exponents depend only on the dimensionality of the manifold.

PACS numbers: 02.30.Sa, 02.10.Yn, 05.45.Mt

1. Introduction

In a recent work on general properties of complete metric spaces [1] Vershik introduced
specific types of random matrices, which he called distance matrices, and asked questions
about their statistical properties.

Distance matrices are defined for any metric space X with some probability measure on it
in the following way. Consider N points randomly distributed on X according to the measure.
The matrix element M_{ij} of the $N \times N$ (real symmetric) distance matrix M equals the distance
on X between points i and j. In all cases considered here, it is tacitly assumed that there
always exists a distance $\| \ldots \|$ on X between two points i and j which depends only on their
relative position and we use the notation

$$M_{ij} = \|\vec{x}_i - \vec{x}_j\| \tag{1}$$

where $\vec{x}_i$ is the d-dimensional vector locating the point i on X, and d is the dimension of the
base manifold.

For any realization of the random points, (real) eigenvalues Λ_n and eigenvectors $u^{(n)}$ of
distance matrices are well defined,

$$\sum_{j=1}^{N} M_{ij} u_j^{(n)} = \sum_{j=1}^{N} \|\vec{x}_i - \vec{x}_j\| u_j^{(n)} = \Lambda_n u_i^{(n)}. \tag{2}$$

We are interested in their statistical properties.

The first quantity to be considered is the average eigenvalue density defined as

$$\rho(\Lambda) = \left\langle \frac{1}{N} \sum_{j=1}^{N} \delta(\Lambda - \Lambda_j) \right\rangle \tag{3}$$

or equivalently the average integrated eigenvalue density, i.e. the average staircase function

$$\mathbf{N}(\Lambda) = \left\langle \frac{1}{N} \sum_{j=1}^{N} \Theta(\Lambda - \Lambda_j) \right\rangle. \tag{4}$$

Here $\langle \ldots \rangle$ denotes an average taken over realizations. $N\mathbf{N}(\Lambda)$ (counting function) counts the number of eigenvalues up to the value Λ.

As the elements of distance matrices are non-negative there is one large positive eigenvalue whose existence follows from the Perron–Frobenius theorem (see e.g. [2] vol 2, p 49). When the metric space X is Euclidean or spherical all other eigenvalues have the remarkable property of being non-positive (the counting function associated with a distance matrix satisfies $\mathbf{N}(0^+) = (N - 1)/N$). The proof of this for Euclidean spaces is given in [3] (see [4] for a general discussion of the subject). The purpose of the present paper is the investigation of the asymptotics, in the limit of a large number of points N, of the average eigenvalue density at large and small negative eigenvalues and the properties of the corresponding eigenfunctions for distance matrices built from a uniform distribution of uncorrelated points on a base manifold.

The plan of the paper is as follows. In section 2 one-dimensional spaces are considered in detail. In section 2.1 we demonstrate that the case of the interval is equivalent to the one-dimensional Anderson model with diagonal disorder. Though all states are localized, the localization length increases for large negative eigenvalues as discussed in section 2.2. When the localization length is much larger than the system size, the concept of localization becomes meaningless and a plane wave description of such states is adequate. This happens for large negative eigenvalues and as shown in section 2.3 it leads to a power-law behaviour of the eigenvalue density. For small negative Λ, states are strongly localized and in section 2.4 it is demonstrated that in the one-dimensional case the eigenvalue density tends to a constant. The properties of the participation ratio are also discussed in this section.

When instead of the interval the circle is considered, two new phenomena appear. First, as demonstrated in section 3, the delocalized eigenvalues corresponding to large negative Λ form quasi-doublets whose splittings are much smaller than the distance among them. Second, as shown in section 3.1, the localized eigenfunctions of the distance matrix on the circle are, in general, localized not in one but in two diametrically opposite regions (forming a kind of echo).

In section 4 d-dimensional spaces are investigated. First in section 4.1 we introduce the continuous approximation valid for large negative eigenvalues and show that it leads to a $|\Lambda|^{-(2d+1)/(d+1)}$ asymptotics of the average eigenvalue density. In section 4.2 it is demonstrated that if the base manifold has a symmetry group, large negative eigenvalues of its distance matrix form quasi-multiplets whose dimensions equal the dimensions of the irreducible representations of the group. For small $|\Lambda|$, the splitting of these multiplets becomes comparable to the distance among them and the quasi-multiplet structure disappears. The general condition for the applicability of the continuous approximation is discussed in section 4.3 where it is demonstrated that the quasi-multiplets are present only for the first $\sqrt{N}$ largest negative eigenvalues. In section 4.4 the behaviour of the average eigenvalue density for strongly localized states is investigated and it is shown that it vanishes as $|\Lambda|^{d-1}$. To investigate eigenfunction properties the participation ratio is considered in the same section. The presence of a localization echo is also established for higher dimensions.

Numerical calculations when the points are distributed uniformly on spheres and cubes of different dimensions are consistent with the results found.

2. One-dimensional spaces

2.1. Distance matrices on an interval

Let us consider N uncorrelated points x_j distributed uniformly on an interval of length L. The distance matrix in this case is

$$M_{ij} = |x_i - x_j| \tag{5}$$

where $|\dots|$ stands for the usual modulus. The eigenvalue equation (2) reads

$$\sum_{j=1}^{N} |x_i - x_j| u_j = \Lambda u_i \qquad \text{for} \quad i = 1, \dots, N. \tag{6}$$

The eigenvalues of distance matrices are insensitive to the ordering of the N points but the understanding of the structure of the eigenvectors depends heavily on it. We will rearrange the points x_j in increasing order

$$0 \leqslant x_1 \leqslant x_2 \leqslant \cdots \leqslant x_N \leqslant L. \tag{7}$$

Subtract equations (6) with indices $i + 1$ and i (assuming (7)), then

$$\Lambda(u_{i+1} - u_i) = \sum_{j=1}^{N} (|x_{i+1} - x_j| - |x_i - x_j|) u_j. \tag{8}$$

As

$$|x_{i+1} - y| - |x_i - y| = (x_{i+1} - x_i) \begin{cases} -1 & \text{when} \quad y \geqslant x_{i+1} \\ 1 & \text{when} \quad y \leqslant x_i \end{cases} \tag{9}$$

one obtains

$$\Lambda(u_{i+1} - u_i) = (x_{i+1} - x_i) \left[-\sum_{j=1}^{i} u_j + \sum_{j=i+1}^{N} u_j \right]. \tag{10}$$

After simple manipulations one proves that these equations are equivalent to

$$\Lambda(R_{i+1} - 2R_i + R_{i-1}) = 2(x_{i+1} - x_i) R_i \tag{11}$$

where $R_i = L_i - L_N/2$ with $L_i = \sum_{j=1}^{i} u_j$ for $i = 1, \dots, N$ and $L_0 = 0$.

This second-order difference equation has to be completed with boundary conditions. The first follows from the definition of R_i,

$$R_N = -R_0. \tag{12}$$

The second one can be obtained from any of equations (6) by expressing u_i through L_i. Combining equations (6) with $i = 1$ and $i = N$ one obtains

$$\Lambda(-R_1 - 2R_N + R_{N-1}) = 2(x_1 - x_N) R_N. \tag{13}$$

This condition can be cast in the form of equations (11) by introducing the point $x_{N+1} = x_1$. Then equations (11) are valid for all $i = 1, \dots, N+1$ and the boundary conditions correspond to the anti-symmetric solutions

$$R_N = -R_0 \qquad R_{N+1} = -R_1. \tag{14}$$

Equations (11) coincide with the one-dimensional Anderson model

$$R_{i+1} - (E - V_i)R_i + R_{i-1} = 0 \qquad \text{for} \quad i = 1, \ldots, N+1 \tag{15}$$

with diagonal disorder

$$E - V_i = 2\left(1 + \frac{l_i}{\Lambda}\right) \tag{16}$$

where l_i ($=x_{i+1} - x_i$) are random variables equal to the distance between adjacent points. When $N \to \infty$ and the points x_j are uncorrelated, l_i are independent random variables with the Poisson distribution

$$P(l) = \bar{\rho}\,e^{-\bar{\rho}l} \tag{17}$$

where

$$\bar{\rho} = \frac{N}{L} \tag{18}$$

is the mean density of initial points.

2.2. Localization length

It is well known (see e.g. [5]) that all solutions of the one-dimensional Anderson model (15) are exponentially localized, i.e. they have asymptotically the following decay from their maximum value, say at n_0,

$$|R_n| \sim e^{-|n-n_0|/l_{\text{loc}}} \tag{19}$$

where l_{loc} is the dimensionless localization length.

When $|\Lambda| \to \infty$ the fluctuating part of the random potential (16) tends to zero and it is convenient to use the perturbation theory developed in [6]. The first terms of the expansion of the localization length for the one-dimensional Anderson model (15) with a random potential ϵV of zero mean ($\langle V \rangle = 0$) are

$$\frac{1}{l_{\text{loc}}} \approx \epsilon^{2/3} \left[\sqrt{x} - \frac{\langle V^2 \rangle}{8x} \right] \tag{20}$$

where $E - 2 = \epsilon^{4/3}x$. In our case $\epsilon = 1/(\Lambda\bar{\rho})$, $V_i = 2(l_i\bar{\rho} - 1)$, and $x = 2\epsilon^{-1/3}$. By introducing the dimensionless scaled eigenvalue

$$\lambda = \bar{\rho}\Lambda = \frac{N}{L}\Lambda \tag{21}$$

one has

$$\frac{1}{l_{\text{loc}}} \approx \sqrt{\frac{2}{\lambda}} - \frac{1}{4\lambda}. \tag{22}$$

This expression is valid for positive λ. When λ is negative the first term is imaginary and only the second term remains,

$$l_{\text{loc}} \to -4\lambda \qquad \text{when} \quad \lambda \to -\infty. \tag{23}$$

2.3. Crystal configuration

Though for the model (15) all states are formally localized, only N sites exist in our problem and, as usual for finite systems, the effect of localization can be ignored when the change of the wavefunction over the system size is small

$$\frac{N}{l_{\text{loc}}} \ll 1. \tag{24}$$

For large N equation (23) indicates that states with $|\lambda| \geqslant N/4$ are practically delocalized and all states with smaller $|\lambda|$ are localized.

For delocalized states, the fluctuating part of the potential (16) is unimportant. Neglecting it is equivalent to investigating the spectrum of the distance matrix for an equally spaced point configuration

$$x_i = \frac{i}{N+1} L \qquad \text{for} \quad i = 1, \ldots, N \tag{25}$$

which we call the crystal configuration. From equation (15) it follows that for this configuration the R_i take an especially simple form

$$R_i = aq^i + bq^{-i} \tag{26}$$

where q is related to the scaled eigenvalue λ,

$$\lambda = \frac{2q}{(1-q)^2}. \tag{27}$$

The allowed values of q (and consequently of λ) are determined from the boundary conditions (14). Straightforward calculations give two equations for q,

$$q^N + 1 = 0 \tag{28}$$

$$q^{N+1} + 1 = \frac{N+1}{N-1}(q^N + q). \tag{29}$$

The set of solutions of both equations (except $q = -1$) corresponds to eigenvalues of the crystal distance matrix. If q is a solution then $1/q$ is also a solution and both give the same eigenvector and eigenvalue, and the total number of solutions is N, as it should be.

These equations have only one real solution that gives the Perron–Frobenius (i.e. the largest positive) eigenvalue. All other solutions have the form $q = e^{i\phi}$ and correspond to a negative value of λ,

$$\lambda = -\frac{1}{2\sin^2 \phi/2}. \tag{30}$$

For large N, solutions of equations (28) and (29) have the form

$$q = e^{u/N} \tag{31}$$

with u independent on N. The corresponding eigenvalues are

$$\lambda = \frac{1}{2\sinh^2(u/2N)} \to \frac{2N^2}{u^2} \qquad \text{when} \quad N \to \infty. \tag{32}$$

In this limit equation (29) takes the form

$$\cosh z = z \sinh z \tag{33}$$

where $z = u/2$. Its unique positive real solution is $z \approx 1.199\,68$ and the Perron–Frobenius eigenvalue $\lambda \sim 1.6671N^2$. The imaginary solutions $u = i\phi$ of equation (29) lead to the following asymptotics $\phi = 2(\pi n - 1/(\pi n)) + O(n^{-2})$. Together with the solutions of equation (28) $\phi = (2m+1)\pi$ the allowed values of ϕ are approximately $\phi_n \to \pi n$, with $1 \ll n \ll N$ and the corresponding scaled eigenvalues are

$$\lambda_n = -\frac{2N^2}{\pi^2 n^2}. \tag{34}$$

The counting function $\mathbf{N}(\lambda)$ of large negative eigenvalues is

$$\mathbf{N}(\lambda) = \frac{1}{N} \sum_{n=1}^{N} \Theta(\lambda - \lambda_n) \to \frac{C}{(-\lambda)^{1/2}} \tag{35}$$

with $C = 4\sqrt{2}/\pi$.

The $N \to \infty$ behaviour of the crystal configuration distance matrix can also be obtained without knowledge of the exact solution by noting that in this limit the eigenvector components u_j can be replaced by a continuous function $u(x)$ with x as in equation (25). In this approximation (which we call the continuous approximation) the eigenvalue equation (6) takes the form

$$\Lambda u(x) = \frac{N}{L} \int_0^L |x - y| u(y) \, \mathrm{d}y. \tag{36}$$

Differentiating this equation twice and taking into account that $|x|'' = 2\delta(x)$, one obtains

$$\Lambda u''(x) = 2 \frac{N}{L} u(x). \tag{37}$$

Its general solution is $u(x) = a \, \mathrm{e}^{vx} + b \, \mathrm{e}^{-vx}$, with $\Lambda = 2N/(v^2 L)$. Substituting it in equation (36) one obtains equations for a and b whose compatibility conditions are exactly equations (28) and (33).

The conditions of applicability of the continuous approximation are discussed in section 4.3.

2.4. Strongly localized states

Strongly localized states with small eigenvalues correspond to the configuration of points x_j in which two points, say x_1 and x_2, are separated by a distance $r = |x_1 - x_2|$ much smaller than the mean distance between points $\bar{\rho} r \ll 1$. Let u_1 and u_2 be the eigenvector components at points x_1 and x_2. The eigenvalue equation (6) gives

$$\Lambda u_1 = r u_2 + \sum_{j \neq 1,2} |x_1 - x_j| u_j \qquad \Lambda u_2 = r u_1 + \sum_{j \neq 1,2} |x_2 - x_j| u_j. \tag{38}$$

As $x_1 \approx x_2$ the sums above are approximately equal and by subtracting these equations one obtains that to leading order in $\bar{\rho} r$

$$\Lambda = -r. \tag{39}$$

Starting from this value of Λ it is possible to build a perturbation theory in higher powers of $\bar{\rho} r$.

Therefore, each time there exist two points anomalously close to each other, a strongly localized state with the eigenvalue (39) is formed. The density of such states is equal to the probability that two uncorrelated points are separated by a small distance $r = -\Lambda$. From equation (17) it follows that at negative $\lambda = \bar{\rho} \Lambda$

$$\rho(\lambda) \sim \mathrm{e}^{\lambda}. \tag{40}$$

Strictly speaking equation (40) is applicable only for very small λ and it indicates that in the one-dimensional case $\rho(\lambda)$ tends to a constant when $\lambda \to 0$.

A convenient way to distinguish between localized and delocalized states is to compute the participation ratio $\mathbf{R}$,

$$\mathbf{R} = \frac{\left(\sum_{j=1}^{N} u_j^2 \right)^2}{\sum_{j=1}^{N} u_j^4}. \tag{41}$$

When an eigenfunction is delocalized, all u_j are of the same order and the participation ratio N increases linearly with N, $\mathbf{R} \sim N$. For strongly localized states the participation ratio is independent of N and $\mathbf{R} \sim l_{\mathrm{loc}}$. Therefore, when the number N of points is fixed, the
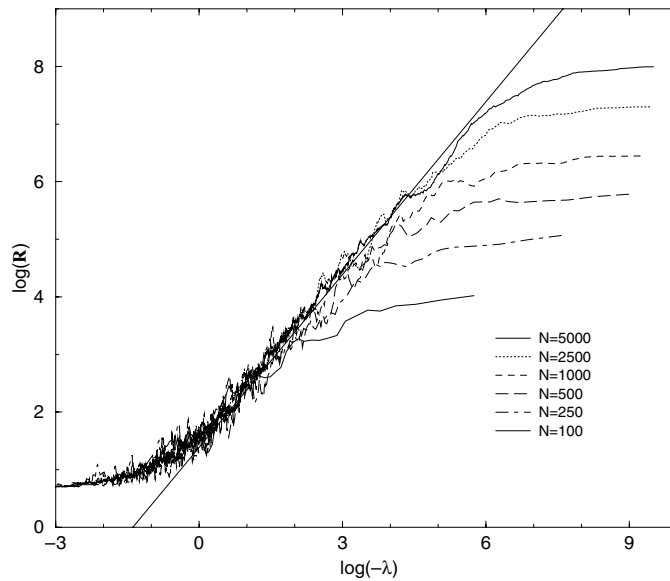
Figure 1. Participation ratio corresponding to a single realization for the unit interval smoothed over a small window of $\delta\lambda$ with different number N of points. Straight line: asymptotics (23) of the localization length, for comparison.

participation ratio as function of the corresponding eigenvalue is a constant (proportional to N) till it becomes equal to the localization length and ceases to depend on N.

In figure 1 the results for the participation ratio from numerical simulations are displayed and the expected behaviour is clearly seen. **R** is constant and proportional to N far from the origin (on the right-hand side of the figure), and curves corresponding to different N coalesce to the localization length when approaching the origin (towards the left of the figure).

3. Distance matrices on the circle

The distance between two points (i and j) on a manifold is defined as the length of the shortest geodesic connecting them. For later discussion, it is convenient to distinguish between two kinds of manifolds. We shall call a manifold for which there exists a single geodesic connecting two points a manifold of the first kind and of the second kind otherwise. The simplest examples of this classification are provided by the interval and the circle for the first and second kind, respectively.

Let us proceed with the case of the circle. For a circle of radius R parametrized by the polar angle φ the distance is

$$\|\varphi_i - \varphi_j\| = R \begin{cases} |\varphi_i - \varphi_j| & \text{if} \quad |\varphi_i - \varphi_j| \leqslant \pi \\ 2\pi - |\varphi_i - \varphi_j| & \text{if} \quad \pi < |\varphi_i - \varphi_j| \leqslant 2\pi. \end{cases} \tag{42}$$

This equation differs from equation (5) and the arguments of the previous section must be slightly modified, in particular for the crystal configuration consisting of N equally spaced points located at $\varphi_j = 2\pi j/N$. In this case, the distance matrix M takes the form

$$M_{ij} = \|\varphi_i - \varphi_j\| = \frac{2\pi R}{N} f(i - j) \qquad i, j = 1, \ldots, N \tag{43}$$

where $f(k)$ are the integers,

$$f(k) = \begin{cases} k & 0 \leqslant k \leqslant [N/2] \\ N - k & [N/2] < k < N \end{cases} \tag{44}$$

and $[x]$ is the integer part of x. M is therefore a circulant matrix whose successive rows are obtained by cyclic permutations of the first one (see e.g. [7]). Its eigenvectors are the Fourier harmonics

$$u_j^{(n)} = e^{2\pi i n j / N} \qquad n, j = 1, \ldots, N \tag{45}$$

with eigenvalues

$$\Lambda_n = \frac{2\pi}{N} \sum_{k=1}^{N} f(k) \, e^{2\pi i n k / N}. \tag{46}$$

As in the preceding section it is convenient to define the scaled eigenvalues λ as

$$\lambda = \Lambda \frac{N}{2\pi R}. \tag{47}$$

The sum (46) takes a different form for N even or odd. For N even

$$\lambda_n = -\frac{1 - (-1)^n}{2 \sin^2(\pi n / N)} \qquad n = 1, \ldots, N - 1 \quad \lambda_N = \frac{N^2}{4} \tag{48}$$

and for N odd

$$\lambda_n = -\frac{1 - (-1)^n \cos(\pi n / N)}{2 \sin^2(\pi n / N)} \qquad n = 1, \ldots, N - 1 \quad \lambda_N = \frac{N^2 - 1}{4}. \tag{49}$$

The eigenvalues with n and $N - n$ are degenerate due to the fact that both $u_j^{(n)}$ and $u_j^{(n)*} = e^{-2\pi i n j / N}$ are eigenvectors of the distance matrix (43). When $n/N \ll 1$

$$\lambda_n = \lambda_{N-n} \to -(1 - (-1)^n) \frac{N^2}{2\pi^2 n^2} \tag{50}$$

similar to equation (34) for the crystal solution for the interval except for exact two-fold degeneracies for the circle.

As for the distance matrix on the interval, the asymptotic behaviour of eigenvalues with $n/N \to 0$ for the circle can be calculated by considering u_j as a continuous function $u(2\pi j / N)$. In this approximation the eigenvalue equation reads

$$\Lambda u(\varphi) = \frac{NR}{2\pi} \int_0^{2\pi} \|\varphi - \varphi'\| u(\varphi') \, d\varphi'. \tag{51}$$

Taking the second derivative one obtains

$$\Lambda u''(\varphi) = \frac{NR}{\pi} (u(\varphi) - u(\varphi - \pi)). \tag{52}$$

The second term appears due to definition (42) of the distance on the circle when $|\varphi - \varphi'| > \pi$. The periodic solutions of this equation are $e^{\pm i n \varphi}$ with eigenvalues given by (50). Note that for n odd the contribution to equation (51) from angles close to π is the same as the contribution from small angles and for n even they cancel each other.

3.1. Strongly localized states

The behaviour of the eigenvalue density for the distance matrix on the circle is practically the same as on the interval (except for quasi-degenerate doublets). However, strongly localized eigenfunctions for the circle differ from those for the interval. This is in contrast to the familiar situation (e.g. for the Anderson model) in which strongly localized wavefunctions do not depend on the choice of boundary conditions. The origin of this difference is to be found in the (unusual) growth of the matrix elements with the distance.

Let us assume that an eigenfunction is localized in a region L of the order of the localization length l_{loc} with $l_{loc} \ll 1$ and u_i are (large) components of this eigenfunction inside this region. Consider a certain point φ_0 (measured from a point inside L) at a distance larger in comparison with the size of the localization region. Due to localization the value u_0 of the eigenfunction at this point decreases exponentially $|u_0| \sim e^{-|\varphi_0/l_{loc}|}$. On the other hand u_0 has to be computed from equation (2) where the sum can be restricted to points lying in the localization region

$$\Lambda u_0 = \sum_{i \in L} \|\varphi_0 - \varphi_i\| u_i. \tag{53}$$

Let $0 < \varphi_0 - \varphi_i < \pi$. Then

$$\Lambda u_0 = \varphi_0 \sum_{i \in L} u_i - \sum_{i \in L} \varphi_i u_i. \tag{54}$$

As the eigenfunction considered is a localized state, $|u_0|$ should be much smaller than $|u_i|$ for all $\varphi_0 \gg l_{loc}$. But the sums on the right-hand side include only the values of u_i inside L which are (almost) independent of φ_0. Therefore, in order to obey the localization property, the u_i inside the localization region should satisfy

$$\sum_{i \in L} u_i \approx 0 \qquad \sum_{i \in L} \varphi_i u_i \approx 0. \tag{55}$$

Here the sign ≈ 0 means that these sums should be exponentially small ($\sim e^{-|\varphi_0|/l_{loc}}$). When only powers of l_{loc}/φ_0 are considered, the above sums are zero,

$$\sum_{i \in L} u_i = 0 \qquad \sum_{i \in L} \varphi_i u_i = 0 \tag{56}$$

which can be interpreted as conditions for the vanishing of the total charge and the total dipole moment of charges u_i located at φ_i. These are the only general relations to be satisfied for the interval. They do not depend on φ_0 and express the necessary conditions for the vanishing of the eigenfunction outside the localization region.

However, for the circle, a new feature appears when the point φ_0 is close to a region diametrically opposite to the localization region L. In that region $\varphi_0 = \pi + \psi_0$ with $|\psi_0| \ll 1$ and, due to the definition of the distance (42), equation (53) takes the form

$$\Lambda u_0 = \pi \sum_{i \in L} u_i - \sum_{\varphi_i < \psi_0} (\psi_0 - \varphi_i) u_i + \sum_{\varphi_i > \psi_0} (\psi_0 - \varphi_i) u_i. \tag{57}$$

The important difference in equation (54) is that the right-hand side of this equation depends strongly on φ_0 which determines the splitting between negative and positive sums in (57). No simple conditions can be imposed on the values of the eigenfunction inside the localization region (similar to equations (56)) insuring naturally that the left-hand side of equation (57) is small. Consequently, our assumption (required in the usual localization theory) that a circle eigenfunction is localized only in one small region is not correct and the above arguments indicate that eigenfunctions of distance matrices on the circle are, in general, localized not in one but at least in two diametrically opposite regions. Exceptions to this rule may be
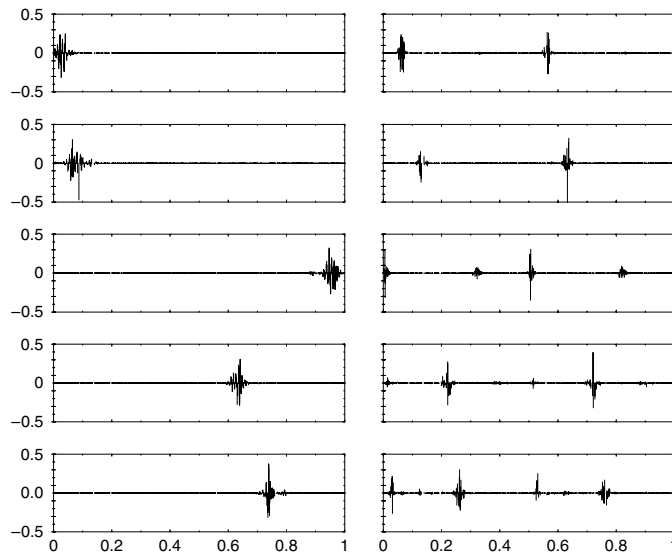
Figure 2. Individual eigenfunctions $u^{(n)}$ corresponding to the nth eigenvalue with $N = 1000$ points on the unit interval (left-hand side) and on the unit circle (right-hand side). From top to bottom: $n = 200, 210, 220, 230$ and 240.

constituted by states localized in such a small region that the diametrically opposite one contains no points (i.e. one of the sums in equation (57) is empty).

In figure 2 numerically calculated eigenfunctions of the distance matrices for the interval and the circle are plotted. In both figures, the abscissa axis is the distance from the origin divided by the total length. As predicted, for the case of the interval (left-hand side) each eigenfunction is localized in one small region whereas for the circle (right-hand side) the eigenfunctions are large in two diametrically opposite regions (regions whose abscissas differ by a value of $\frac{1}{2}$).

Later we will show that the sort of 'echo' discussed here is present, in general, for distance matrices on manifolds of the second kind. Examples are given in the next section.

4. Higher dimensional spaces

In this section we generalize the methods developed for the one-dimensional case to higher dimensional spaces.

4.1. Continuous approximation

The asymptotics of the average eigenvalue density at large negative eigenvalues is related to delocalized states whose contribution can be calculated in the continuous approximation. It is then necessary to solve the following equation,

$$\Lambda u(\vec{x}) = \frac{N}{V} \int_X \|\vec{x} - \vec{y}\| u(\vec{y}) \, d\vec{y} \tag{58}$$

where the points $\vec{x}$ and $\vec{y}$ belong to a d-dimensional base manifold X of volume V.

In a small vicinity of each regular point the manifold can be considered as a part of the d-dimensional Euclidean space R^d with coordinates $\vec{z}$. In such vicinity, eigenfunctions of equation (58) can be considered as functions of $\vec{z}$ and we seek for semiclassical-type solutions

$$u(\vec{z}) \sim e^{i\vec{q}\vec{z}} \tag{59}$$

with a large vector $\vec{q}$.

Locally equation (58) leads to the following expression for the eigenvalues,

$$\Lambda(q) \approx \frac{N}{V} \int_{R^d} |\vec{z}| \, e^{i\vec{q}\vec{z}} \, d\vec{z}. \tag{60}$$

This formula is valid for manifolds of the first kind where two points can be connected by a single geodesic. For manifolds of the second kind (such as spheres) there exist a few regions which will contribute to $\Lambda(q)$. For clarity only the first case will be considered in detail.

Formally, the integral (60) is divergent but it can be computed from the convergent integral

$$I(\alpha, \vec{q}) = \int_{R^d} e^{-\alpha|\vec{z}|} \, e^{i\vec{q}\vec{z}} \, d\vec{z} \qquad (\alpha > 0) \tag{61}$$

by using $\Lambda(q) = -(N/V)\partial I(\alpha, \vec{q})/\partial \alpha|_{\alpha=0}$. The integral (61) can be expressed through the beta function (see e.g. [8] vol 1, 1.5.1) and the final result is

$$\Lambda(q) = -\Omega_{d-1}(d-1)! \frac{N}{V}(q^2)^{-(d+1)/2} \tag{62}$$

where $\Omega_{d-1} = 2\pi^{d/2}/\Gamma(d/2)$ is the volume of the $(d-1)$-dimensional unit sphere $x_1^2 + \cdots + x_d^2 = 1$, and $\Gamma(x)$ is the gamma function.

When the base manifold is a part of the d-dimensional Euclidean space and d is odd, the result (62) can also be obtained by successive differentiation of both sides of equation (58) similar to what was done in section 2.1. In this case, one also obtains exact relations between the eigenfunctions of the distance matrix and those of the Laplacian for $d = 1$, bi-Laplacian for $d = 3$, etc.

For any smooth boundary conditions, the density of solutions of the form (59) is asymptotically the same as for the spectrum of the Laplacian $(\Delta + q^2)\Psi = 0$, given by

$$\rho(q) = V \int_{R^d} \frac{d\vec{k}}{(2\pi)^d} \delta(q - |\vec{k}|) = \frac{V\Omega_{d-1}}{(2\pi)^d} q^{d-1} \tag{63}$$

where V is the volume of the manifold.

From equations (62) and (63) the following estimate of the tail of the integrated density of eigenvalues of distance matrices is obtained,

$$\begin{aligned} \mathbf{N}(\Lambda) &\approx \frac{1}{N} \int_0^\infty \Theta(\Lambda - \Lambda(q))\rho(q) \, dq \\ &= \frac{V\Omega_{n-1}(q(\Lambda))^d}{(2\pi)^d Nd} = C_d \left(\frac{N}{V}\right)^{1/(d+1)} (-\Lambda)^{-d/(d+1)} \end{aligned} \tag{64}$$

where $q(\Lambda)$ is the inverse of the function $\Lambda(q)$ defined in equation (62) and C_d is a constant depending only on the dimensionality of the system.
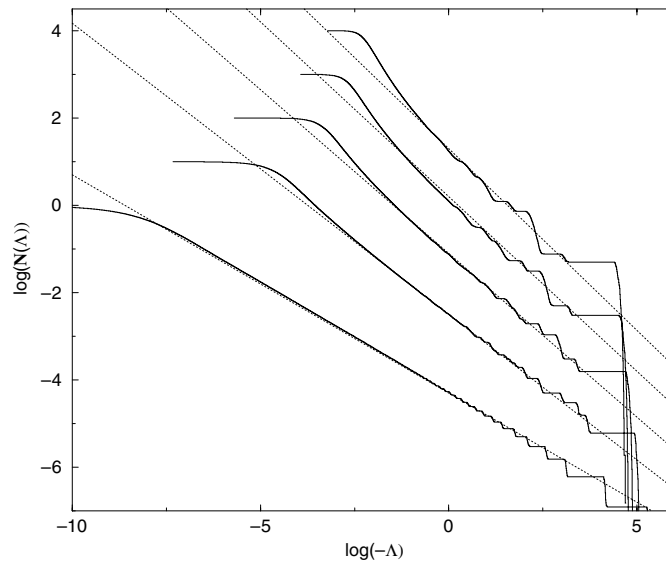
Introducing the dimensionless scaled eigenvalues

$$\lambda = \Lambda \left(\frac{N}{V}\right)^{1/d} \tag{65}$$

this result can be rewritten in the universal form

$$\mathbf{N}(\lambda) \approx C_d(-\lambda)^{-d/(d+1)} \tag{66}$$

where $\mathbf{N}(\lambda)$ is the counting function in the variable λ.

Figure 3. Averaged (over 50 realizations) staircase function with $N = 1000$ points in the unit hyper-cube of dimension $d = 1, 2, 3, 4, 5$ from bottom to top. Straight dotted lines of slope $-d/(d+1)$, as predicted by equation (66), for comparison. For clarity curves are shifted vertically by $d - 1$ units.

For manifolds of the second kind such as spheres, the only modification of the above results is a slight change of the scaled eigenvalue

$$\lambda = \Lambda \left(\frac{gN}{V} \right)^{1/d} \tag{67}$$

where g is the number of singular regions contributing to equation (60). For spheres of arbitrary dimensions $g = 2$.

In figure 3 results of numerical calculations of the average staircase function for hyper-cubes of different dimensions are compared with the prediction (66). They are in very good agreement.

4.2. Quasi-multiplets

The estimates of the previous section are general but they do not take into account the fine structure of the eigenfunctions.

Let us assume that the manifold X is invariant under a certain symmetry group G. As the kernel $\|\vec{x} - \vec{y}\|$ of equation (58) is the distance between two points on this manifold, it remains unchanged under simultaneous transformation of $\vec{x}$ and $\vec{y}$. Therefore from equation (58) it follows that the transformed eigenfunction

$$u'(\vec{x}) = u(G(\vec{x})) \tag{68}$$

is also a solution of this equation. From this simple remark it is clear that in the continuous approximation the eigenfunctions $u(\vec{x})$ form irreducible representations of the symmetry group of the initial manifold similar to solutions of the Laplace equation. When this group has h-dimensional irreducible representations the eigenvalues of distance matrices will be h times degenerate.

To be specific, let us consider in detail the case of the d-dimensional sphere as the base manifold. The invariance group of the sphere is the d-dimensional rotation group. Let $p = d - 1$. It is well known (see e.g. [8] vol 2, 11.2) that the harmonic polynomials of degree $p + 2$ (hyper-spherical harmonics) $Y_{l\vec{m}}(\vec{\theta}, \varphi)$ form the basis of irreducible representations of the rotation group. Here $\vec{\theta} = \theta_1, \ldots, \theta_p$ and φ are the standard hyper-spherical angles and $\vec{m} = m_1, \ldots, m_p$ are integers obeying the inequalities

$$0 \leqslant m_p \leqslant \cdots \leqslant m_1 \leqslant p + 2. \tag{69}$$

The dimensions $h(l, p)$ of these representations are

$$h(l, p) = (2l + p)\frac{(l + p - 1)!}{p!l!} \tag{70}$$

(for $d = 2$, $h(l, 1) = 2l + 1$, and $Y_{lm}(\theta, \varphi)$ are the usual spherical harmonics).

The eigenvalues corresponding to these eigenfunctions have multiplicity $h(l, p)$. Their explicit form can easily be derived directly from the invariance of equation (58) under rotation. Choose the z-axis along the vector $\vec{x}$. Introducing the hyper-spherical coordinates in the usual way, one concludes that $u(\vec{y})$ equals the unique harmonic polynomial depending only on $\cos \theta$ where θ is the angle between vectors $\vec{x}$ and $\vec{y}$ which is proportional to the Gegenbauer polynomial $C_l^{p/2}(\cos \theta)$ (see e.g. [8] vol 2, 11.2). Therefore

$$\Lambda_l = C_{lp}\frac{N}{V} \int_0^\pi \theta C_l^{p/2}(\cos \theta) \sin^p \theta \, d\theta \tag{71}$$

with a constant C_{lp} depending on p and l. The explicit form of Λ_l is not instructive for our purposes.

From properties of the Gegenbauer polynomials (see e.g. [8] vol 2, 10.9) it follows that all Λ_l with even $l \neq 0$ are zero and consequently beyond the reach of the continuous approximation (see section 4.3). The value corresponding to $l = 0$ is the Perron–Frobenius eigenvalue. We therefore concentrate on odd values of l.

In the continuous approximation, the eigenvalues for d-dimensional spheres are $h(2k + 1, d - 1)$ times degenerate. For the one-dimensional sphere (i.e. the circle) $h(2k + 1, 0) = 2$ as in section 3. For the 2-sphere (the usual sphere) $h(2k + 1, 1)$ equals $3, 7, 11 \ldots$, for the 3-sphere the first multiplicities are $4, 16, 36, \ldots$, for the 4-sphere they are $5, 30, 91, \ldots$, etc. In general, the first multiplet for the d-sphere corresponding to $l = 1$ has multiplicity $d + 1$, i.e. it is equal to the dimension of the embedded space. In figure 4 these degeneracies can be read off from the numerically calculated average staircase function for spheres of different dimensions.

We also show in figure 5 the structure of some individual eigenstates. We proceed as follows. Given an eigenvector u, choose its largest (in absolute value) component, say u_1, and plot the components u_j as a function of the distance $\|\vec{x}_1 - \vec{x}_j\|$ (normalizing to the maximum distance between two points on the manifold). By construction, the highest component corresponds to the zero value of the abscissa. For the one-dimensional case, this procedure corresponds to the natural ordering of points on the interval or the circle. The quasi-multiplet structure of the eigenstates is clearly visible in the figure. For comparison, the Perron–Frobenius eigenstate is also displayed. For spheres its components are constant to within $1/\sqrt{N}$ fluctuations.

4.3. Condition for applicability of the continuous approximation

The continuous approximation is based on the well-known fact that under quite general conditions the sum of a large number of independent random variables $\vec{x}_j$ with distribution $d\mu(\vec{x})$ tends to its mean value
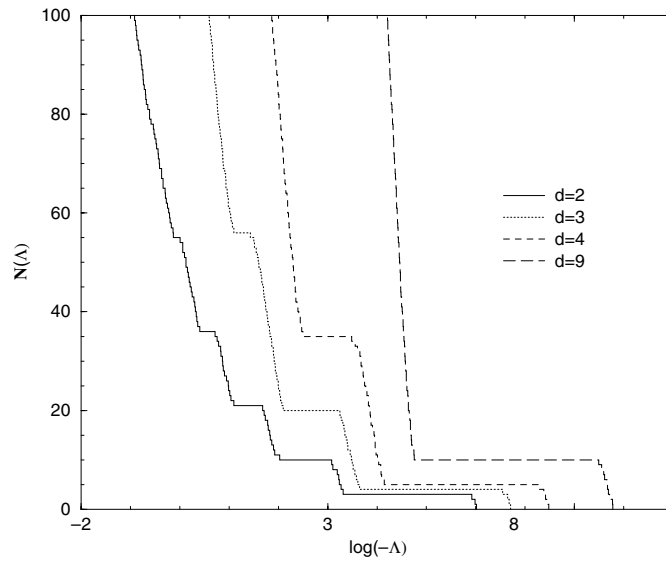
Figure 4. Averaged staircase function with $N = 1000$ points on the d-dimensional unit sphere ($d = 2, 3, 4, 9$) showing quasi-degenerate multiplets. For clarity, the counting function has been normalized to N.
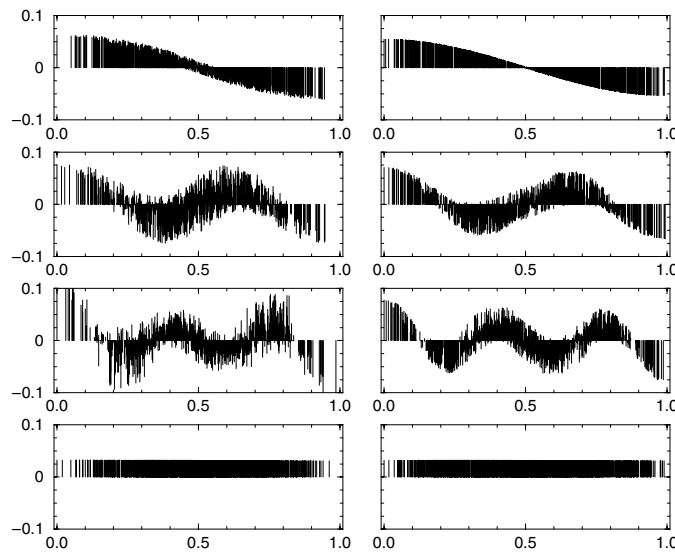
Figure 5. Individual eigenfunctions $u^{(n)}$ corresponding to the nth eigenvalue with $N = 1000$ points on the unit 3-sphere (left-hand side) and on the unit 2-sphere (right-hand side). From top to bottom: $n = 1, 5$ and 21 for $d = 3$ and $n = 1, 4$ and 11 for $d = 2$. These values of n correspond to the lowest eigenvalue of each of the first three quasi-multiplets. The Perron–Frobenius eigenfunction ($n = 1000$) is at the bottom. See text for further explanation.

$$\frac{1}{N} \sum_{j=1}^{N} f(\vec{x}_j) = \int f(\vec{x}) \, d\mu(\vec{x}) + \frac{\zeta}{\sqrt{N}} \tag{72}$$

where, when $N \to \infty$, ζ is a random variable with zero mean and variance independent of N.

This type of 'ergodic theorem' makes it natural to consider, instead of the true eigenvalue equation (2),

$$\tilde{\Lambda}_n u_i^{(n)} = \frac{1}{N-1} \sum_{j=1}^{N} \|\vec{x}_i - \vec{x}_j\| u_j^{(n)}$$ (73)

its continuous approximation

$$\tilde{\Lambda}_n^{(c)} u_n(\vec{x}) = \frac{1}{V} \int_X \|\vec{x} - \vec{y}\| u_n(\vec{y}) \, d\vec{y}$$ (74)

(we introduce for convenience the factor $1/(N-1)$ with the corresponding redefinition $\tilde{\Lambda}_n = \Lambda_n/(N-1)$ because in the sum in (73) there are only $N-1$ non-zero terms). Here for simplicity uncorrelated points $\vec{x}_j$ uniformly distributed on the base manifold X (i.e. $d\mu(\vec{x}) = d\vec{x}/V$) are considered.

As the kernel of the integral equation (74) is symmetric, its eigenvalues $\tilde{\Lambda}_n^{(c)}$ are real and its eigenfunctions $u_n(\vec{x})$ can be chosen real orthogonal,

$$\frac{1}{V} \int_X u_n(\vec{x}) u_m(\vec{x}) \, d\vec{x} = \delta_{mn}.$$ (75)

Let us first consider the case when the eigenvalue $\tilde{\Lambda}_n^{(c)}$ of the continuous equation (74) is non-degenerate and let us look for solutions of the true eigenvalue equation (73) in the form

$$u_j^{(n)} = u_n(\vec{x}_j) + \sum_{m \neq n} c_m u_m(\vec{x}_j)$$ (76)

where c_m are considered as small quantities. (This procedure is often used in perturbation theory when dealing with the Schrödinger equation.) Substituting these expressions in equation (73), multiplying both sides by $u_n(\vec{x}_i)$, and summing from $i = 1$ to N one obtains

$$\tilde{\Lambda}_n \frac{1}{N} \sum_{i=1}^{N} u_n(\vec{x}_i) \left(u_n(\vec{x}_i) + \sum_{m \neq n} c_m u_m(\vec{x}_i) \right)$$
$$= \frac{1}{N(N-1)} \sum_{i,j=1}^{N} u_n(\vec{x}_i) \|\vec{x}_i - \vec{x}_j\| \left(u_n(\vec{x}_j) + \sum_{m \neq n} c_m u_m(\vec{x}_j) \right).$$ (77)

The mean values of the terms that are multiplied by c_m are zero and, consequently, they are of the order of $1/\sqrt{N}$ (see equation (72)). Therefore in equation (77) these terms can be ignored to first order in $1/\sqrt{N}$ and this equation is reduced to

$$\tilde{\Lambda}_n A_N(n) = B_N(n)$$ (78)

where

$$A_N(n) = \frac{1}{N} \sum_{i=1}^{N} u_n(\vec{x}_i) u_n(\vec{x}_i)$$ (79)

$$B_N(n) = \frac{1}{N(N-1)} \sum_{i,j=1}^{N} u_n(\vec{x}_i) \|\vec{x}_i - \vec{x}_j\| u_n(\vec{x}_j).$$ (80)

When $N \to \infty$ these sums tend to their mean value plus corrections

$$A_N(n) \to 1 + \frac{\sigma(n)}{\sqrt{N}} \qquad B_N(n) \to \tilde{\Lambda}_n^{(c)} + \frac{\Sigma(n)}{\sqrt{N}}.$$ (81)

The mean value of $\sigma(n)$ and $\Sigma(n)$ is zero. When $N \to \infty$ their variances are independent on N and can be computed from straightforward calculations.

By taking the average of $A_N(n)$ and $B_N(n)$ one recovers the continuous approximation result. The first correction $\delta\Lambda_n = \tilde{\Lambda}_n - \tilde{\Lambda}_n^{(c)}$ is determined by their fluctuating part

$$\delta\Lambda_n = \frac{1}{\sqrt{N}}\left(\Sigma(n) - \tilde{\Lambda}_n^{(c)}\sigma(n)\right). \tag{82}$$

The mean value of $\delta\Lambda_n$ is, of course, zero and its variance is equal to

$$\langle\delta\Lambda_n^2\rangle = \frac{\tilde{\Lambda}_n^{(c)2}}{N}v^2(n) \tag{83}$$

where

$$v^2(n) = \int_X u_n^4(\vec{x})\,\mathrm{d}\mu(\vec{x}) - 1 \tag{84}$$

provided that the $u_n(\vec{x})$ are orthogonal. For semiclassical-type solutions (59), where real orthogonal solutions can be chosen in the forms $\sqrt{2}\sin\vec{q}\vec{z}$ and $\sqrt{2}\cos\vec{q}\vec{z}$, $v^2(n) = 5$, independent of n.

If the eigenvalue $\tilde{\Lambda}_n^{(c)}$ of the continuous equation (74) is h-fold degenerate, a simple extension of the previous arguments leads to an estimate of the splitting of the degeneracy by including the next order corrections.

Let $u_n^{(m)}(\vec{x})$, $m = 1, \ldots, h$, be the solutions of the continuous equation (74) corresponding to an h-fold degenerate eigenvalue $\tilde{\Lambda}_n^{(c)}$ normalized as follows:

$$\int_X u_n^{(m)}(\vec{x})u_n^{(m')}(\vec{x})\,\mathrm{d}\mu(\vec{x}) = \delta_{mm'}. \tag{85}$$

The total splitting $\Delta\Lambda_n = \sum_{j=1}^h \delta\Lambda_n^{(j)}$ is a random variable which has the following estimate,

$$\frac{\Delta\Lambda_n}{\tilde{\Lambda}_n^{(c)}} = h \cdot \zeta \cdot \frac{v(n)}{\sqrt{N}} \tag{86}$$

with $\langle\zeta\rangle = 0$ and $\langle\zeta^2\rangle = 1$ and

$$v^2(n) = \frac{1}{h^2}\sum_{m=1}^h\sum_{m'=1}^h \int_X \left[u_n^{(m)}(\vec{x})u_n^{(m')}(\vec{x})\right]^2\,\mathrm{d}\mu(\vec{x}) - 1. \tag{87}$$

More generally, if a function $f(\Lambda_n)$ is computed in the continuous approximation, it will have a random (depending on realizations) fluctuation $\delta f(\Lambda_n)$ which to first order in $1/\sqrt{N}$ is

$$\delta f(\Lambda_n) = \frac{\mathrm{d}f(\Lambda_n)}{\mathrm{d}\Lambda_n}h\Lambda_n\zeta\frac{v(n)}{\sqrt{N}}. \tag{88}$$

We are interested mainly in the counting function. According to equation (66) it has a power-law asymptotics when smoothed over a small window $\delta\Lambda$ and $\mathrm{d}\mathbf{N}(\Lambda)/\Lambda = \nu\mathbf{N}(\Lambda)/\Lambda$ with $\nu = -(d+1)/d$. Consequently

$$\delta\mathbf{N}(\Lambda) \sim \mathbf{N}(\Lambda)\frac{\zeta}{\sqrt{N}}. \tag{89}$$

The condition that perturbed eigenvalues do not deviate from those computed in the continuous approximation (or equivalently that the splitting (83) is much smaller than the distance between multiplets in the continuous approximation) leads to the following inequality:

$$\delta\mathbf{N}(\Lambda) \ll \frac{1}{N}. \tag{90}$$

Together with (89) it implies that, in general, the continuous approximation gives correctly the eigenvalues of only the first $\sqrt{N}$ eigenstates ordered by increasing eigenvalues and that by increasing N more and more distinct and isolated multiplets are present. In terms of scaled eigenvalues, one has that the continuous approximation can be used for the approximation of non-averaged eigenvalues satisfying

$$|\lambda| \geqslant N^{(d+1)/2d}. \tag{91}$$

For smaller $|\lambda|$ the spacing between successive eigenvalues computed in the continuous approximation becomes comparable to the fluctuating corrections and the mixing of different states is important.

Nevertheless, one can still use the continuous approximation for the calculation of average quantities (e.g. the counting function). The main point is that the first correction to (89) vanishes because the mean value of ζ is zero to first order in $1/\sqrt{N}$. If there are no singularities (which is probably true for $d > 2$), the next order correction will be of the order of $G(\lambda)/N$ with a certain function $G(\lambda)$ and the conditions (90) on average will be valid till λ is of the order of 1. Therefore for averaged quantities one can use the continuous approximation for a finite fraction of the total number of eigenvalues.

4.4. Strongly localized states

The properties of strongly localized states can be estimated by slightly modifying the arguments used for the one-dimensional case.

For manifolds of the second kind (as for the circle), assume that an eigenfunction is localized in a small region L and u_i are (large) values of this eigenfunction inside this region. Choose the origin somewhere inside this region and consider a point $\vec{x}_0$ at a large distance from it. The value u_0 of the eigenfunction at this point from equation (2) is

$$\Lambda u_0 = \sum_{i \in L} \|\vec{x}_0 - \vec{x}_i\| u_i. \tag{92}$$

As $\|\vec{x}_0\| \gg \|\vec{x}_i\|$, the right-hand side of this expression can be expanded into powers of $\vec{x}_i$,

$$\Lambda u_0 = R \sum_{i \in L} u_i + \sum_{i \in L} \vec{\zeta} \cdot \vec{x}_i u_i + \cdots \tag{93}$$

where $R = \|x_0\|$ and $\vec{\zeta} = \partial \|\vec{x}_0\| / \partial \vec{x}_0$.

As $|u_0|$ should decrease exponentially with R and each term in the above equation decreases as a different power of R, one concludes, similar to the case of the circle, that in order to obey the localization property u_i should obey the relations

$$\sum_{i \in L} u_i \approx 0 \qquad \sum_{i \in L} \vec{\zeta} \cdot \vec{x}_i u_i \approx 0 \quad \text{etc.} \tag{94}$$

In regions not too close to a region diametrically opposite to the localization region $\vec{\zeta} = \vec{x}_0/R$ and these equations take the form of zero multipole moments

$$\sum_{i \in L} u_i = 0 \qquad \sum_{i \in L} \vec{x}_i u_i, \ldots. \tag{95}$$

But close to the diametrically opposite region there are points for which the distance changes its form as in equation (42). For these points the derivative of $\|\vec{x}\|$ will change sign and, in general, it will be impossible to fulfil conditions (95). Consequently, the eigenfunction in the diametrically opposite region cannot, in general, be exponentially small as required by the usual localization theory.
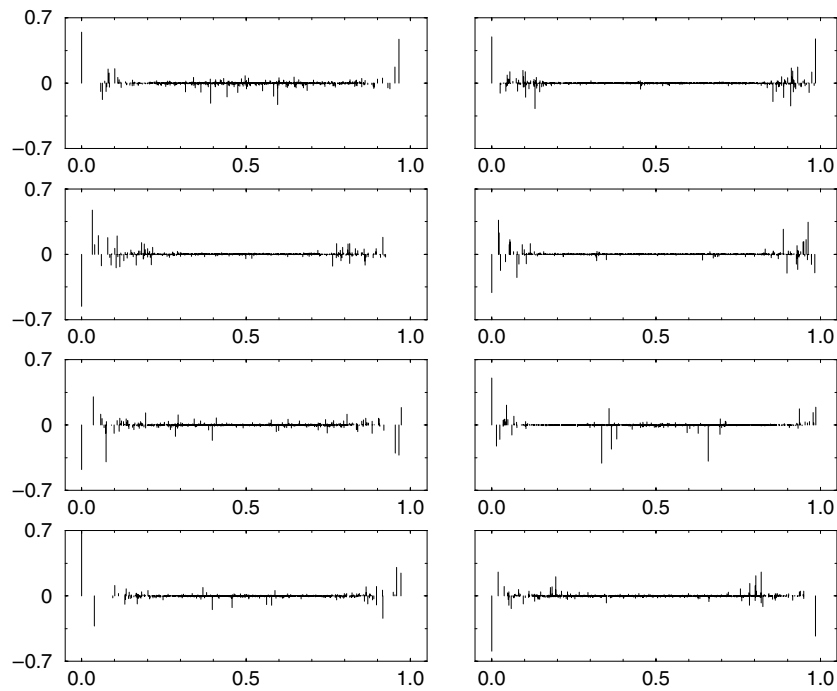
Figure 6. Individual eigenfunctions $u^{(n)}$ as for figure 5 except $n = 800, 801, 802, 803$ for $d = 3$ and $n = 650, 651, 652, 653$ for $d = 2$ from top to bottom. All states are localized.

The above discussion about the localization 'echo' is valid for manifolds of the second kind (i.e. if there exist a few geodesics connecting two points), e.g. for spheres of different dimensions. In figure 6 we present the structure of the localized eigenfunctions of the distance matrices for two- and three-dimensional spheres in the same way as was done in figure 5. In all cases, the eigenfunctions have large values near the left and right ends of the interval, in agreement with localization on two diametrically opposite regions. Comparison with figure 5 also illustrates the completely different structure of extended and localized states (note the difference in scale in both figures).

To compute the density of strongly localized states let us, as above, assume that an eigenfunction is localized in a small region L and denote by u_i its large components inside L. (For simplicity we consider only manifolds of the first kind.)
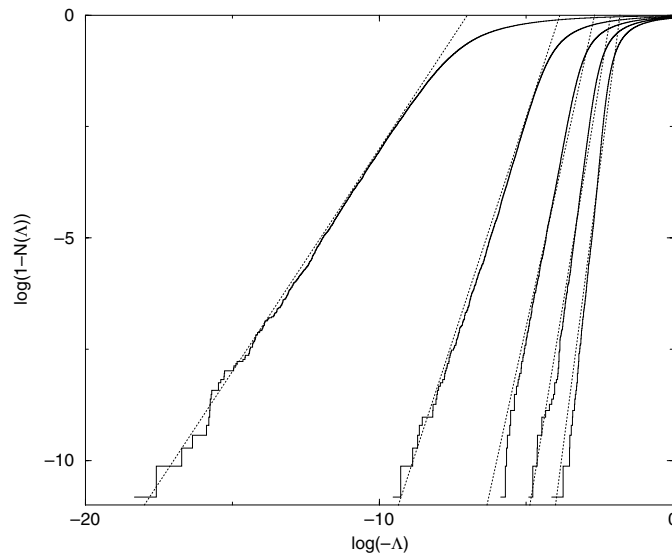
The eigenvalue equation (2) gives

$$\Lambda u_i = \sum_{j \in L} \|\vec{x}_i - \vec{x}_j\| u_j. \tag{96}$$

Because we assume that all u_i are localized (are large) in a small region, all differences $\|\vec{x}_i - \vec{x}_j\|$ are of the order of the distance r between nearest points

$$\Lambda u_i \approx r \sum_{j \neq i} u_j. \tag{97}$$

As already indicated in equation (94), one of the necessary conditions of localization is

$$u_i + \sum_{j \neq i} u_j = 0. \tag{98}$$

Figure 7. Averaged fraction of eigenvalues above Λ with $N = 1000$ points in the unit hyper-cube of dimension $d = 1, 2, 3, 4, 5$ (from left to right). Straight lines of slope d as predicted by equation (100), for comparison.

Therefore

$$\Lambda \approx -r \tag{99}$$

which means that the distribution of eigenvalues of localized states is approximately the same as the distribution of distances between two uncorrelated points randomly distributed on the manifold. For small distances the latter is proportional to the volume and, consequently, the staircase function at small negative λ is

$$\mathbf{N}(\lambda) \approx 1 - K_d(-\lambda)^d \tag{100}$$

where K_d is a constant depending on the dimensionality of the system. (In a situation where points though uniformly distributed exhibit level repulsion we expect the exponent in equation (100) to be larger.)

In figure 7 (same numerical data as for figure 3) the small Λ behaviour of the staircase function is displayed. It is clear that the estimate (100) is in good agreement with the numerical simulations.

Equations (100) and (66), which govern the small and large λ behaviour of the average staircase function respectively, strongly suggest that $\mathbf{N}(\lambda)$ is independent of the number of points N when $N \to \infty$. This is illustrated in figure 8.

To get further insight into localization properties let us first recall some qualitative properties of the Anderson model. In one dimension all states are localized, irrespective of the size of disorder. In two dimensions, perturbation theory cannot be applied and the localization length increases exponentially when disorder decreases. For dimensions greater than two, there is a localization–delocalization transition at finite strength of disorder and the threshold value increases with dimensionality of the system. For distance matrices, the parameter governing the size of the disorder is the scaled eigenvalue $\lambda = \Lambda(N/V)^{1/d}$, with increasing disorder as $|\lambda| \to 0$. In figure 9 we present the numerically computed participation ratio for spheres of dimensions two and three. For the 3-sphere the effect of the
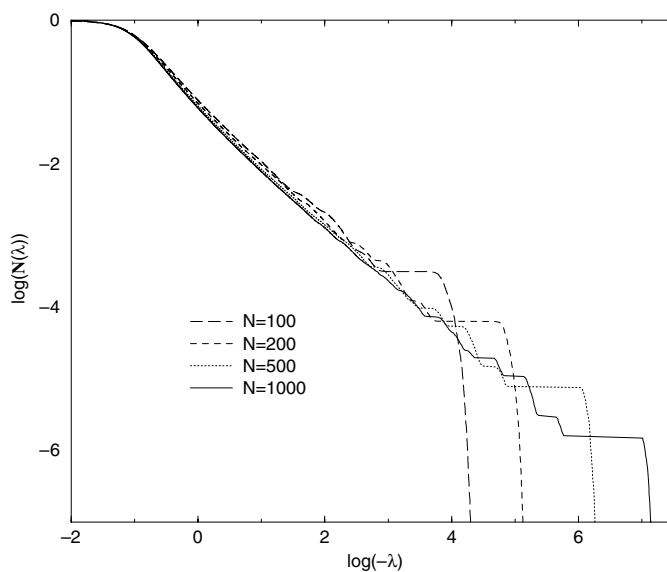
Figure 8. Averaged staircase function for the unit three-dimensional cube for different number of points.
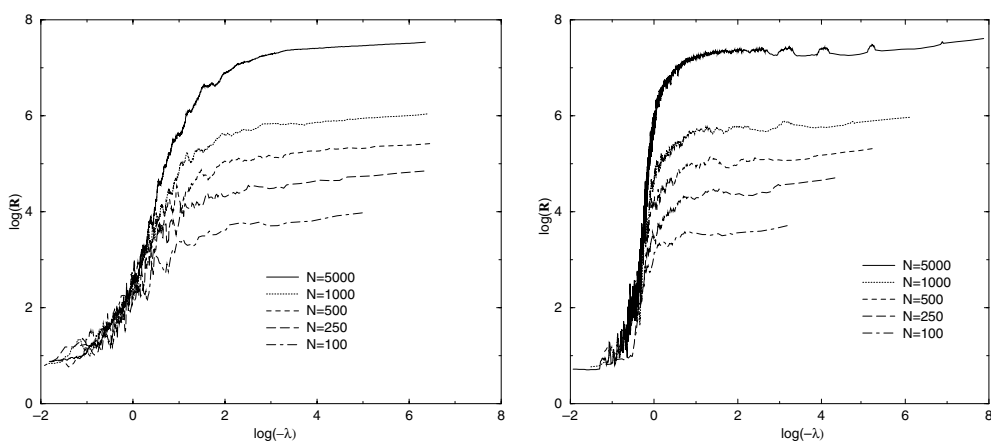
Figure 9. Participation ratio corresponding to a single realization for two-dimensional (left) and three-dimensional (right) unit spheres smoothed over a small window $\delta\lambda$ with different number N of points. The abscissa axis is $\log(-\lambda)$ where $\lambda = \Lambda N^{1/2}$ (left) and $\lambda = \Lambda N^{1/3}$ (right).

localization–delocalization transition (i.e. the sharp increase of the localization length at a finite value of λ) is clearly visible.

5. Summary and conclusions

Let N points be distributed on a certain manifold. The (i, j) matrix element of the distance matrix is defined as the distance between points i and j. Schoenberg [3] proved a long time ago that for Euclidean manifolds all eigenvalues of such matrices, except one, are non-positive.

This property can be extended to other manifolds, in particular to spherical manifolds treated here (see [4] for a general discussion).

The study of the one-dimensional case (interval and circle) already provides some clues as to what are the ingredients governing the properties in higher dimensions and the properties related to the very simple crystal configuration are partially kept when 'disorder' is added.

In general it is demonstrated that, if the points are uncorrelated and uniformly distributed on a base manifold, the average density of eigenvalues of distance matrices in the limit $N \to \infty$ has a power-law behaviour for large and small negative eigenvalues, the exponent depending only on the dimension of the manifold (see equations (66) and (100)).

The eigenfunctions of the distance matrices with large negative eigenvalues are delocalized (for one- and two-dimensional manifolds the localization length is much larger than the system size) whereas the eigenfunctions with very small negative eigenvalues are strongly localized.

If the manifold possesses a symmetry group, large negative eigenvalues form almost degenerate multiplets whose dimensions equal the dimensions of the irreducible representations of the group and the conditions for the presence of isolated multiplets are established.

A distinction among base manifolds for which two points are connected by one or several geodesics is made. In the latter case the eigenfunctions of the distance matrix are, in general, localized not in one but in several regions (echo). For spheres of any dimension, we find strongly localized states in two diametrically opposite regions. The understanding of the structure of the echo for more general spaces deserves further study.

Strongly localized states are, by definition, mostly sensitive to local properties of the base manifold. The existence of the echo shows, however, that certain global properties of the manifold are reflected on these states also.

What proceeds is illustrated in detail by studying distance matrices of uncorrelated points uniformly distributed on hyper-spheres and hyper-cubes of different dimensions.

The introduction of distance matrices in [1] was motivated to a large extent by the fact that they encode the metric properties of the base manifold. Our results show one possible way of solving the inverse problem, namely, the reconstruction of the initial manifold from knowledge of the spectral properties of its distance matrix. We demonstrate that large negative eigenvalues can be approximated with $1/\sqrt{N}$ accuracy by the solutions of the continuous approximation (58). As this integral equation is similar to the Laplace equation, one may conjecture that for this equation, similarly as for the former, the question raised by Kac 'Can one hear the shape of a drum?' [9] can also be answered affirmatively, except probably for very special isospectral cases.

When completing this work we became aware of [10] where Euclidean random matrices were introduced. Matrix elements are then a function of the finite range of the relative distance between two points in Euclidean space $M_{ij} = f(\|\vec{x}_i - \vec{x}_j\|)$. One of the main differences with respect to the present work is that in [10] the results strongly depend on the choice of f whereas here it is kept fixed, $f(x) = x$, and emphasis is put on the choice of the manifold.

Acknowledgments

References

[1] Vershik A M 2002 Distance matrices, random metrics and Urysohn space *Preprint* MPIM Bonn math.GT/ 0203008
[2] Gantmacher F R 1966 *Théorie des Matrices* vol 1 and 2 (Paris: Dunod)
[3] Schoenberg I J 1937 On certain metric spaces arising from euclidean spaces by a change of metric and their imbedding in Hilbert space *Ann. Math.* **38** 724–38
[4] Bogomolny E, Bohigas O and Schmit C Distance matrices and isometric embedding, to be published
[5] Lifshits I M, Gradeskul S A and Pastur L 1987 *Introduction to the Theory of Disordered Systems* (New York: Wiley)
[6] Derrida B and Gardner E 1984 Lyapunov exponent of the one-dimensional Anderson model: weak disorder expansions *J. Physique* **45** 1283–95
[7] Mehta M L 1989 *Matrix Theory, Selected Topics and Useful Results* (Les Ulis: Les Editions de Physique)
[8] Erdélyi A (ed) 1953 *Higher Transcendental Functions* (New York: McGraw-Hill)
[9] Kac M 1966 Can one hear the shape of a drum? *Am. Math. Mon.* **73** 1–23
[10] Mézard M, Parisi G and Zee A 1999 Spectra of Euclidean random matrices *Nucl. Phys.* B **559** 689–701